Adsorption 9: 265–274, 2003

An Experimental and Theoretical Study of the Performance of a Continuous Counter-Current Adsorber

DIANA S.C. PHELPS AND DOUGLAS M. RUTHVEN
Department of Chemical Engineering, University of Maine, Orono, ME 04469-5737, USA
druthven@umche.maine.edu

Abstract. The performance of a simple counter-current adsorber based on the endless belt concept has been studied for vapor phase operation, using as a model system the adsorption of CO_2 from N_2 on a silicalite adsorbent. For this system the isotherm is essentially linear. The steady-state performance can be represented either by the Kremser equation or on a McCabe-Thiele operating diagram. The system is equivalent to 3–8 theoretical stages, depending on to the flow conditions, and both the steady-state and transient behavior are reasonably well predicted by this model. Under properly selected operating conditions it is possible to obtain a reduction in the CO_2 concentration by a factor of 100.

Keywords: counter-current adsorption, CO_2-N_2 separation, silicalite, moving bed

Introduction

In a previous publication (Phelps and Ruthven, 2002) we presented the results of an experimental study of a simple type of counter-currrent adsorbent contactor based on the principle of the endless belt. That study was carried out for a liquid phase system and it was shown that, as a consequence of the internal liquid re-circulation caused by the hydrodynamic drag of the belt, the system behaved, under most conditions, as a single theoretical stage. Since the re-circulation problem should be less severe in the gas phase we decided to carry out a similar study for an appropriately selected vapor phase system. To meet the practical constraints imposed by the apparatus requires a system in which the adsorption isotherm is close to linear under ambient conditions, with a Henry constant that is not so large as to prevent the adsorbent being regenerated by isothermal purging rather than by thermal or vacuum swing. The adsorption of CO_2 from a nitrogen carrier onto silicalite fulfills the basic requirements and this was therefore selected as an appropriate model system.

The objective of this study was to explore the performance and thus to assess the practical potential of this type of adsorption system for vapor phase operation.

Apparatus

The experimental set-up is shown in Fig. 1. The actual contactor was the same as that used for the liquid phase study but it was fitted with a different adsorbent belt and appropriately modified auxiliary equipment. The contactor contains two equivalent sections, separated by mercury seals through which the belt circulates continuously. The fluid flows through the two sections are independent but in normal operation both sections are operated under conditions of counter-current flow, as sketched in Fig. 1(b).

The feed stream contained 10% CO_2 in a N_2 carrier and the flow rate was controlled by a mass flow controller. A pure N_2 stream controlled by a second mass flow controller served as the desorbent purge stream. The compositions of extract and raffinate streams were measured using two Gow-Mac thermal conductivity detectors the signals from which were digitized and passed to a personal computer where they were recorded using VISIM software. The flow rates

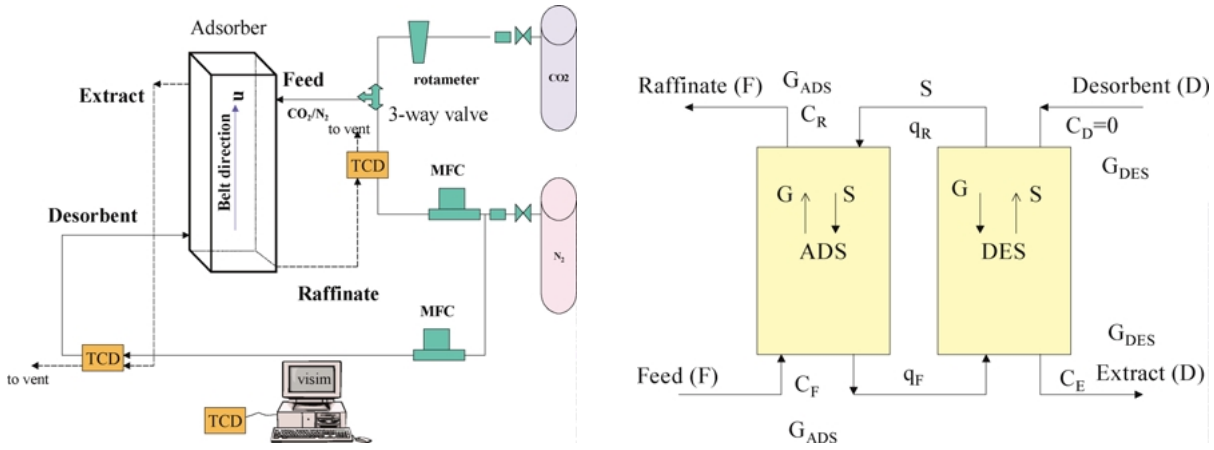

(a) (b)

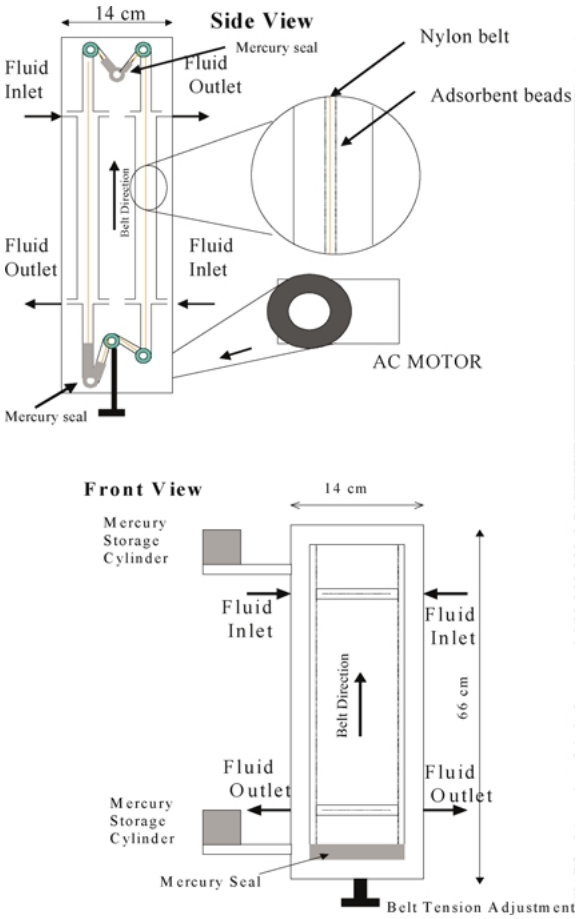

(c)

Figure 1. Experimental apparatus. (a) The actual flow schematic. (b) Formal representation as two "back to back" counter-current contactors. (c) Details of the actual contactor.

of extract and raffinate stream were monitored on rotameters before venting to a fume hood.

The adsorbent belt was made from a woven nylon mesh (10.2 cm wide and 147.5 cm long) coated with crushed silicalite adsorbent (UOP HISIV3000) 30–70 mesh size fraction. The adsorption equilibrium isotherm for CO_2 is shown in Fig. 2. It is evident that the isotherm is essentially linear up to about 150 Torr CO_2 pressure.

Measurement of Adsorbent Capacity

To measure the adsorptive capacity of the belt we carried out a series of pulse measurements (CO_2 injected into a N_2 stream) at several different flow rates. A similar series of measurements carried out with an uncoated belt yielded the dead volume. For the uncoated belt the mean retention time is given by:

$$\tau = \frac{V_d + V}{F} = \frac{\int_0^\infty ct\,dt}{\int_0^\infty c\,dt} \tag{1}$$

where V represents the active volume of the system between the inlet and outlet connection and V_d represents the dead volume associated with the piping, entry and exit sections (between injection valve and detector). The active volume (V) can be calculated reasonably accurately from the dimensions of the system ($V = 300$ cm^3) so the volume of V_d (=100 cm^3) may be obtained by difference.

For the coated (stationary) belt:

$$\tau = \frac{V_d}{F} + \frac{V}{F}\left(1 + \frac{Kw}{l}\right) = \frac{\int_0^\infty ct\,dt}{\int_0^\infty c\,dt} \tag{2}$$

where w/l represents the ratio of the adsorbent thickness to the half-thickness of the duct. The velocity of propagation of the pulse is given by:

$$\omega = \frac{L}{\left(\tau - \frac{V_d}{F}\right)} = \frac{\bar{v}}{1 + Kw/l} \tag{3}$$

where $\bar{v} = F/A$ and $V = LA$. Values of ω calculated from the measured retention times (Eq. (2)) are plotted against the average fluid velocity ($\bar{v}$) in Fig. 3. The relationship is evidently linear, as expected, and from the slope of this plot we find $Kw/l = 1.87$.

Theoretical Considerations

The performance of a counter-current mass transfer device may be conveniently represented as a McCabe-Thiele operating diagram. Such a diagram for "back to back" adsorption and desorption systems is shown schematically in Fig. 4. The operating lines for the

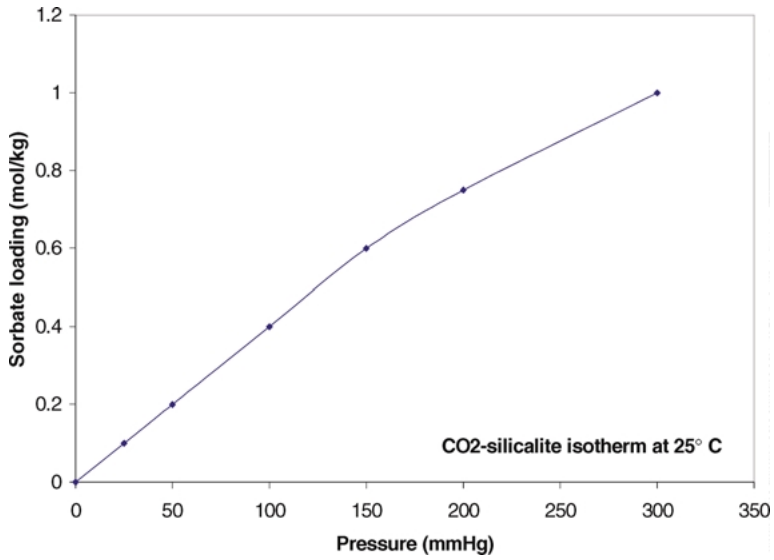

Figure 2. Adsorption equilibrium isotherm for CO_2-silicalite at 25°C. Adapted from Graham et al. (1989).

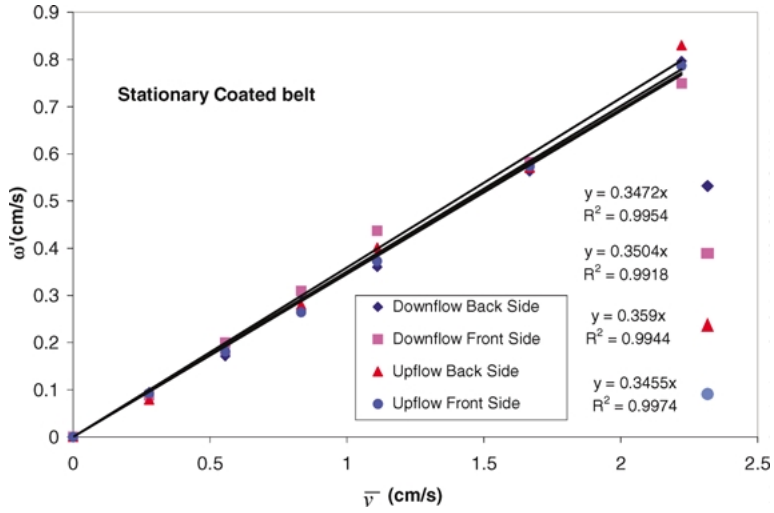

Figure 3. Plot of average wave velocity vs. mean fluid velocity for the system with stationary adsorbent belt.

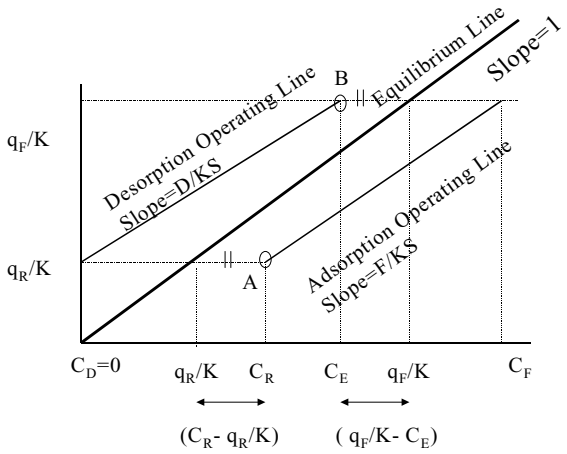

Figure 4. McCabe-Thiele operating diagram for a "back to back" adsorption system of the type sketched in Fig. 1.

adsorption and desorption section fall on opposite sides of the equilibrium line. Equivalently, for a linear system, the performance may be predicted from the Kremser Eq. (3):

$$\text{Adsorption:}\quad \frac{C_R - q_R/K}{C_F - q_R/K} = \frac{A-1}{A^{N+1}-1} \equiv f(A)$$
$$\text{Desorption:}\quad \frac{q_F - KC_F}{q_R - KC_F} = \frac{(1/A)-1}{(1/A)^{N+1}-1} \equiv f(1/A) \tag{4}$$

where $A = KS/G = (Kw/l)(u/\bar{v})$.

If the desorbent rate is sufficiently high so that essentially complete regeneration is achieved ($q_R \to 0$) the maximum removal of sorbate will be achieved (for any given value of A). Under these conditions:

$$\frac{C_R}{C_F} \approx \frac{A-1}{A^{N+1}-1} \tag{5}$$

For a symmetric system with equal flow rates in the adsorption and desorption sections ($G = F = D$) it follows by material balance that $C_E = C_F - C_R$. Combining this relation with Eq. (4) yields an expression for the effectiveness of sorbate removal from the feed stream:

$$\frac{C_R}{C_F} = \frac{f(A) + f(1/A)}{1 + f(1/A)} \tag{6}$$

The performance of such a system is thus seen to be governed by the two parameters A and N. The functional dependence, calculated from Eq. (5) is shown in Fig. 5. When N is greater than about 6 the plot of C_R/C_F vs. A passes through a minimum at $A \approx 1.0$–1.5.

A further useful inequality constraint can be derived by considering the material balance. If $F = D$, the slopes of the operating lines must be the same. Furthermore the points A and B (Fig. 4) must lie on opposite sides of the equilibrium line so:

$$\frac{q_F - q_R}{C_E - C_R} > K \tag{7}$$

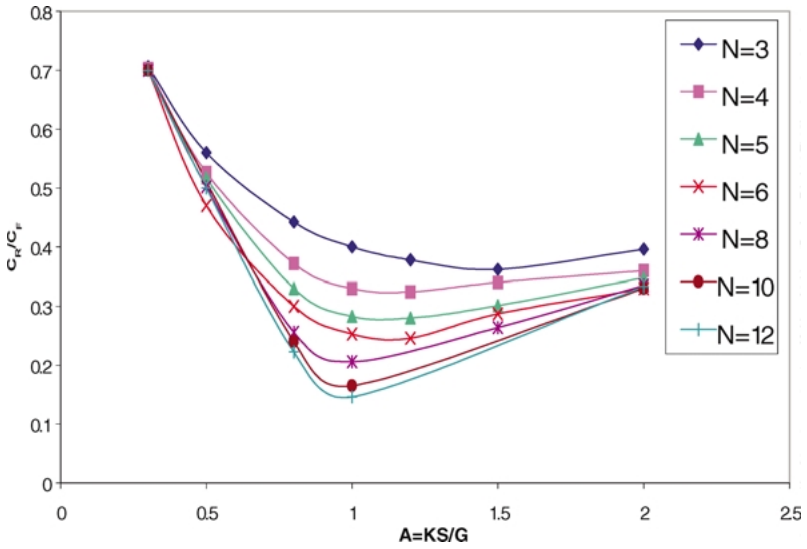

Figure 5. Variation of raffinate concentration with parameter $A\ (=KS/G)$ for different values of N calculated from Eq. (6).

i.e. the slope of line AB (Fig. 4) must be greater than that of the equilibrium line.

Also:

$$(q_F - q_R) = \frac{G}{S} C_E \tag{8}$$

So we obtain the conditions:

$$\begin{aligned} \frac{G}{KS} &> \left(1 - \frac{C_R}{C_E}\right) \quad (\text{when } D = F) \\ \frac{D}{KS} &> \left(1 - \frac{C_R}{C_E}\right) \quad (\text{when } D > F) \end{aligned} \tag{9}$$

Steady State Experiments

A series of experiments was made at different flow conditions (feed rate, desorbent rate and belt speed). When steady state was reached the concentrations of raffinate feed and extract streams were measured. The data so obtained are summarized in Table 1, in which only those runs which satisfy the basic mass balance constraints given by Eq. (9) have been retained.

In Fig. 6 the concentration ratio (C_R/C_F) is plotted against $A[=(K\,w/l)(u/\bar{v})]$ for those runs for which desorbent and feed rates are the same $(D = F)$. The

Table 1. Summary of experimental steady state runs.

$C_F = 10\%\ CO_2/90\%\ N_2$ $A = 6\ cm^2$				(%CO_2) out		CO_2 pick up (cm^3/min)		$G/KS > 1 - C_R/C_E$ $F/KS = D/KS$			
Run no.	F (cm^3/min)	D (cm^3/min)	u (cm/s)	C_R	C_E	Feed side	Des. side	C_R/C_F	$1 - C_R/C_E$	F/KS	D/KS
1	100	1000	0.5	0.11	1.01	9.9	10.18	0.01	0.89	0.29	2.91
2	200	200	0.1	5.73	4.27	9.12	8.93	0.57			
3	200	200	0.5	2.54	6.47	15.31	13.84	0.25	0.60	0.60	0.69
7	200	400	0.5	1.08	4.39	18.04	18.36	0.11	0.75	0.59	1.19
8	200	800	0.5	0.57	2.14	18.97	17.51	0.06	0.73	0.52	2.31
9	200	1000	0.5	0.19	1.76	19.66	17.96	0.02	0.89	0.57	3.16
15	400	800	0.5	2.16	3.62	32.07	30.04	0.22	0.40	1.06	2.31
17	600	600	1	2.52	6.68	46.04	42.94	0.25	0.38	0.67	0.75
21	800	800	1	3.15	5.1	56.58	43.02	0.32	0.38	0.86	0.86
22	800	800	2	3.4	6.05	54.64	51.5	0.34	0.44	0.58	0.63
23	800	800	3	3.78	6.05	51.71	51.5	0.38	0.38	0.48	0.49

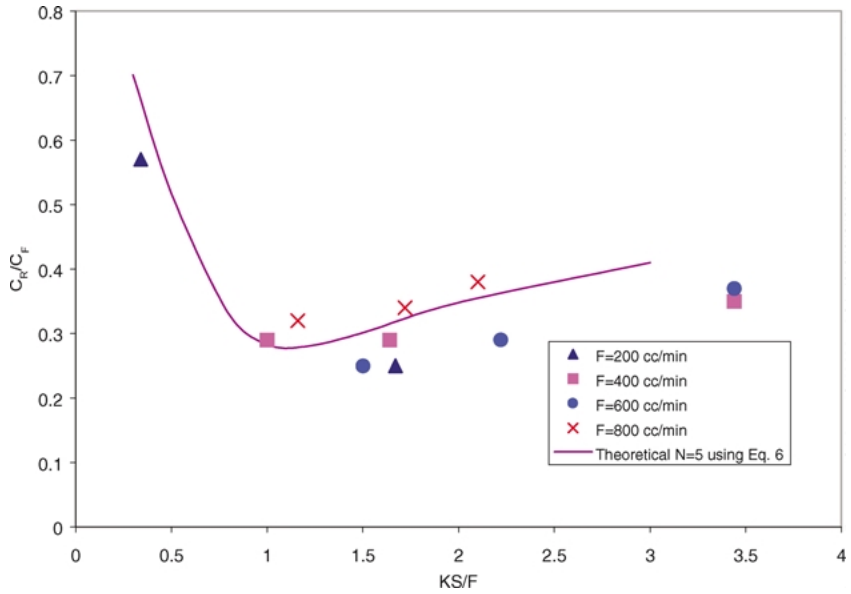

Figure 6. Experimental data showing the variation of the ratio C_R/C_F with KS/G for those runs for which $D = F$. The theoretical curve calculated from Eq. (5) with $N = 5$ is also shown.

qualitative form of this plot is similar to Fig. 5 indicating that, in conformity with Eq. (6), the concentration ratio depends mainly on the velocity ratio $u/\bar{v}$ rather than on the individual values of the u or $\bar{v}$. The performance of the system can be represented approximately as equivalent to five theoretical stages. Exact conformity with this simple model is not to be expected since the height equivalent to a theoretical plate depends to some extent on u and $\bar{v}$.

The effects of operating at a high desorbent feed ratio is illustrated by runs 1, 10 and 9, all of which show efficient removal of CO_2 from the feed stream (C_R/C_F small). Assuming complete regeneration of the adsorbent runs 1 and 10 correspond to approximately 4.5 theoretical stages, estimated from Eq. (5).

Representative McCabe Thiele plots are shown in Fig. 7 and the numbers of theoretical stages (for the adsorption side) estimated from both the McCabe Thiele plots and the Kremser equation are summarized in Table 2. The system is evidently equivalent to between 3 and 8 theoretical stages depending on the flow

Table 2. Summary of selected runs showing comparison of number of stages (adsorption side) obtained by different methods.

Run no.	u (cm/s)	C_R/C_F	F (cm^3/min)	D (cm^3/min)	γ_{ads} (KS/F)	N_{mc}	N_{kr}	N_{tr}
1	0.5	0.01	100	1000	3.6	3	–	3
2	0.1	0.57	200	200	0.65	3–4	3	3
3	0.5	0.25	200	200	1.66	5–6	6–7	–
7	0.5	0.11	200	400	1.71	2–3	–	3
8	0.5	0.06	200	800	1.94	6	–	5
9	0.5	0.02	200	1000	1.73	6	–	6
11	0.5	0.29	400	400	0.99	4–5	5	3
12	1	0.29	400	400	1.68	6	6	–
15	0.5	0.22	400	800	0.94	7–8	7–8	–
17	1	0.25	600	600	1.50	5	6–7	–

Where N_{mc} = number of stages obtained by McCabe plot.
N_{kr} = number of stages obtained by Kremser analysis (Fig. 7.4).
N_{tr} = number of stages obtained by transient response analysis.

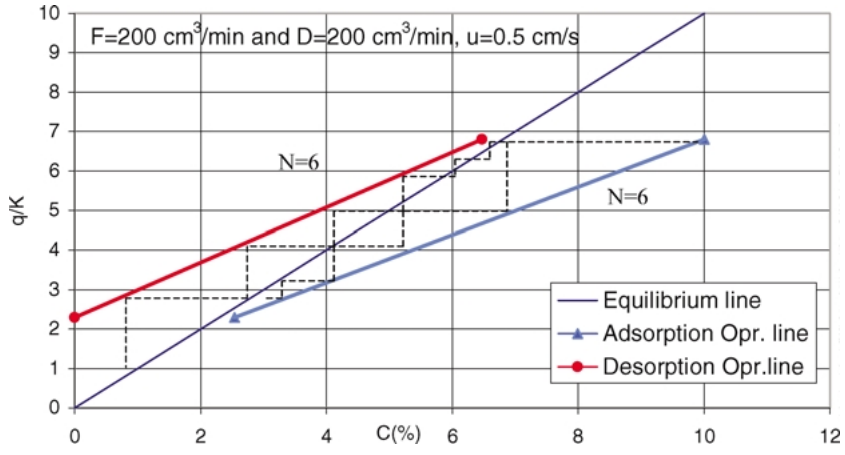

(a)

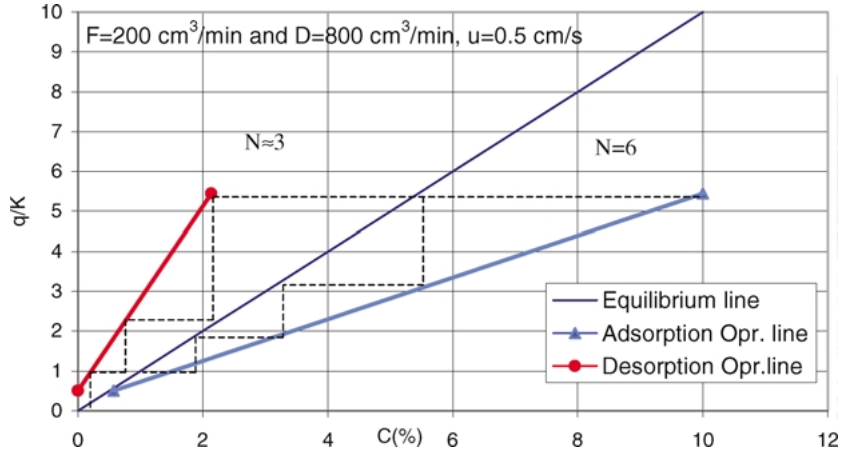

(b)

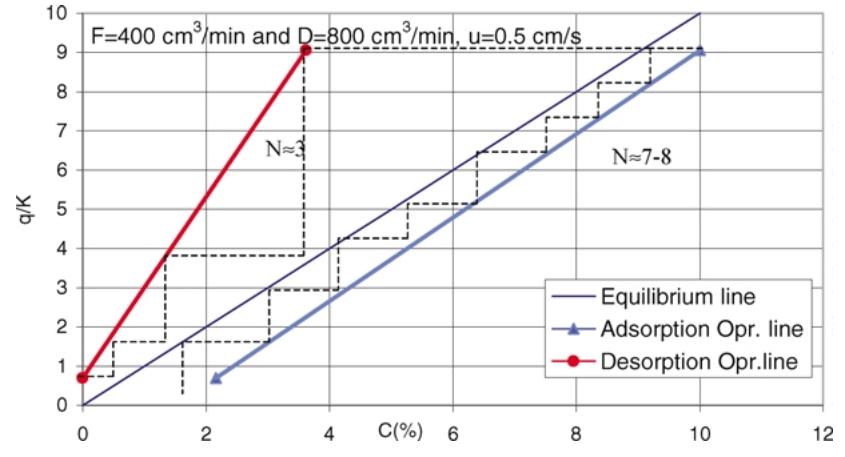

(c)

Figure 7. Mc-Cabe Thiele operating diagrams for representative experimental runs (a) Run 3, (b) Run 8, and (c) Run 15.

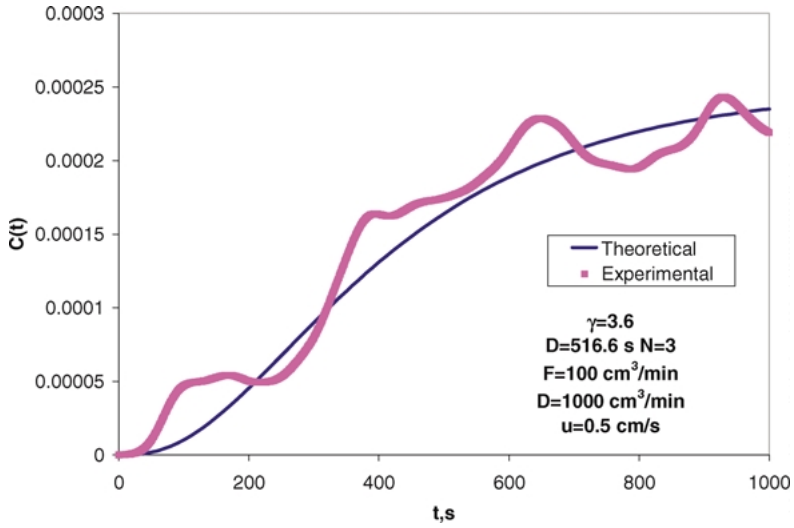
0.0003
0.00025
0.0002
0.00015
0.0001
0.00005
0
C(t)
0
200
400
600
800
1000
t,s
Theoretical
Experimental
γ=3.6
D=516.6 s N=3
F=100 cm3/min
D=1000 cm3/min
u=0.5 cm/s

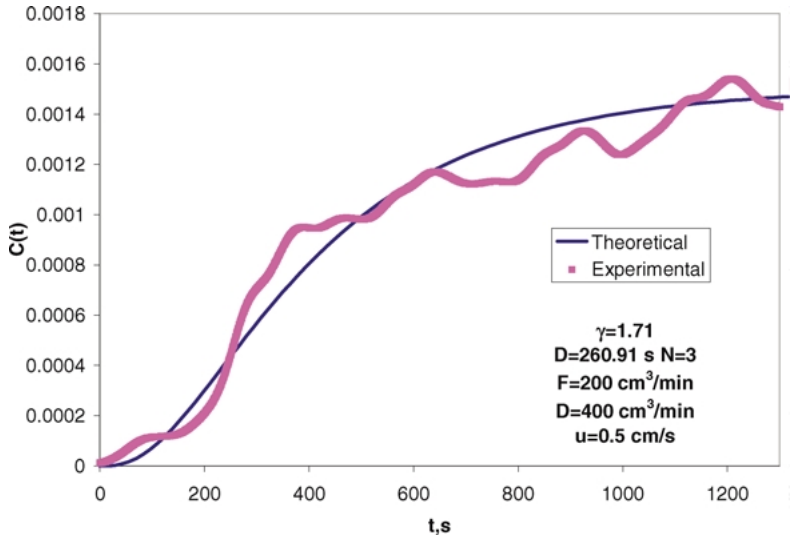
0.0018
0.0016
0.0014
0.0012
0.001
0.0008
0.0006
0.0004
0.0002
0
C(t)
0
200
400
600
800
1000
1200
t,s
Theoretical
Experimental
γ=1.71
D=260.91 s N=3
F=200 cm3/min
D=400 cm3/min
u=0.5 cm/s

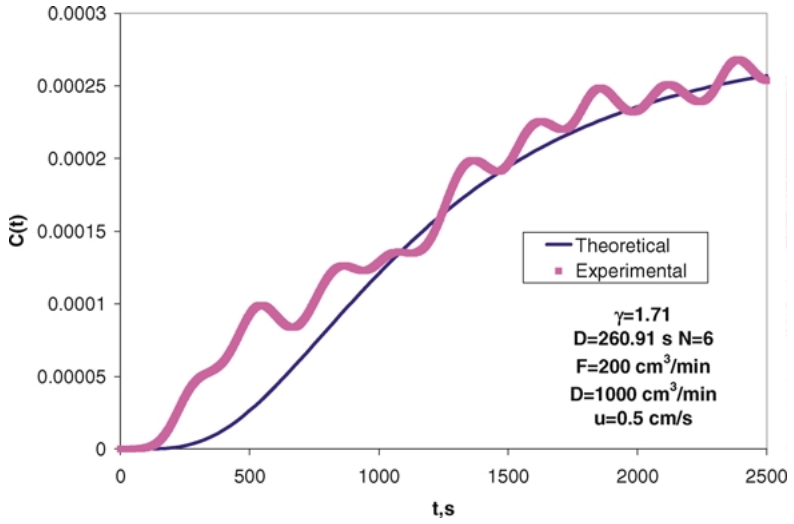
0.0003
0.00025
0.0002
0.00015
0.0001
0.00005
0
C(t)
0
500
1000
1500
2000
2500
t,s
Theoretical
Experimental
γ=1.71
D=260.91 s N=6
F=200 cm3/min
D=1000 cm3/min
u=0.5 cm/s

conditions with the larger numbers corresponding to the higher flow rates.

Transient Behavior

A theoretical model for the transient behavior of a counter-current mass transfer device has been given by Lapidus and Amundson (1950) and this model has been applied to a counter-current adsorption system by Ching and Ruthven (1985). For an initially sorbate free system fed with a well regenerated adsorbent ($q_R = 0$ in Fig. 1(b)) the relevant expressions giving the time dependence of the fluid concentration are:

$$c(t) = \frac{-2\gamma^{\frac{1-N}{2}}}{D(N+1)} c_0 \times \left[\sum_{1}^{N} (-1)^l \sin\left(\frac{\pi l}{N+1}\right)^2 \left(\frac{e^{s_l(t)} - 1}{s_l}\right) \right] \quad (10)$$

where

$$s_l = \frac{-1}{D}\left[\gamma + 1 - 2\sqrt{\gamma}\cos\left(\frac{\pi l}{N+1}\right)\right], \quad l = 1, 2, \ldots, N \quad (11)$$

Since A is known from the retention time measurements ($A = 1.87\beta$) the only unknown is the number of theoretical stages (N).

Transient response curves were generated experimentally by exposing the adsorbent to a step change in CO_2 concentration at time zero while maintaining a high desorbent flow rate to ensure complete regeneration during the desorption step ($q_R = 0$). Representative experimental response curves are shown in Fig. 8. Together with the theoretical curves calculated from Eqs. (10) and (11) with values of N determined by trial and error to provide the best fit. Although the experimental data show some fluctuation it is clear that the model provides a good representation of the system behavior. The values of N derived from the transient measurements which are included in Table 2, are consistent with the values derived from the steady state measurements.

Conclusions

When operated in the liquid phase this type of adsorbent contactor has been shown to behave essentially as a single theoretical stage (Phelps and Ruthven, 2002). This is a consequence of the internal backmixing induced by the hydrodynamic drag of the moving belt. In the vapor phase the viscosity is much lower, resulting in less internal fluid recirculation and less severe backmixing. As a result the mass transfer performance is better. The present system is shown to be equivalent to several theoretical stages and, under properly selected conditions, a concentration reduction ratio (raffinate/feed) of 1/100 can be achieved. This performance is consistent with theoretical expectations based on residence time distribution measurements (Phelps, 2000) which suggest that the HETP is 5–10 cm, depending on the flow conditions. The equilibrium stage model provides a good representation of the experimentally observed performance under both transient and steady-state conditions.

There is some scope for improving the performance by optimizing the design of the system. For example the RTD studies suggest that there is significant backmixing associated with dead volume at the inlet and outlet. This could be reduced by careful redesign, reducing the size of the adsorbent particles and thickness of the adsorbent layer would also help by reducing the resistance to mass transfer but the particles are already quite small (30–70 mesh = 0.04 cm average diameter) and the adsorbent layer is quite thin so the scope for improvement is modest. As a rough estimate it might be possible to reduce the HETP by a factor of two, thus doubling the number of theoretical stages.

In summary this type of contactor can give several theoretical stages within a fairly compact unit using only a small quantity of adsorbent. It has some potential for vapor-phase operation in special situations where a high contacting efficiency is necessary in a compact continuous flow unit. However practical limitations reduce the performance well below what might be anticipated simply from theoretical estimates of the ideal

Figure 8. Transient response of the system when subjected to a step increase in feed concentration at time zero. $C(t)$ represents the effluent concentration in volts. For these runs the desorbent flow rate is high so the entering adsorbent can be considered "clean".

HETP. The sealing problem and the need to maintain balanced pressures present further practical limitations so it is unlikely that this type of system will find any widespread practical application.

Nomenclature

A Kremser equation parameter ($=KS/G$); area
C_D Desorbent concentration
C_E Extract concentration
C_F Feed concentration
C_R Raffinate concentration
c Fluid-phase concentration
c_0 Feed concentration
D Desorbent flow rate; residence time
F Feed flow rate
G Fluid flow rate (feed or desorbent)
K Equilibrium constant
L Length of channel
l Half thickness of channel
N Number of stages
q_i Adsorbed phase concentration
S Adsorbent flow rate
t Time
u Belt speed
V Active volume of the channel (vessel)
V_d Dead volume
$\bar{v}$ Average fluid velocity
w Thickness of belt coating

Greek Letters

β Endless belt adsorber parameter ($u/\bar{v}$)
γ KS/G
ω Wave velocity
τ Average residence time

References

Ching, C.B. and D.M. Ruthven, *Chemical Engineering Science*, **40**, 887 (1985).

Graham, P., A.D. Hughes, and L.V.C. Rees, *Gas Separation and Purification*, **3**, 56 (1989).

Kremser, A. Nat. Pat. News 22,21,42. See also M. Sanders and S.G. Brown. *Ind. Eng. Chem.*, **24**, 214–527 (1932).

Lapidus, L. and N.R. Amundson, *Industrial and Engineering Chemistry*, **42**, 1071 (1950).

Phelps, D.S.C. Ph.D. Thesis, University of Maine, Orono, ME, August 2000.

Phelps, D.S.C. and D.M. Ruthven, "Performance of an Endless Belt Counter-Current Adsorber for Liquid Phase Adsorption," *Separation and Purification Technology*, **27**, 243–256 (2002).